05

The influence of rare-earth metals on glass-forming ability and crystallization of CoFeSiBNb amorphous alloys

© B.A. Rusanov,[1] V.E. Sidorov,[1,2] P. Svec Sr.,[3] D. Janickovic,[3] V.I. Lad'yanov,[4] S.A. Petrova,[2,5] A.A. Sabirzyanov[6]

[1] Ural State Pedagogical University, Ekaterinburg, Russia
[2] Ural Federal University after the first President of Russia B.N. Yeltsin, Yekaterinburg, Russia
[3] Institute of Physics, Slovak Academy of Sciences,
845 11 Bratislava, Slovakia
[4] Udmurt Federal Research Center, Ural Branch Russian Academy of Sciences, Izhevsk, Russia
[5] Institute of Metallurgy of Ural Branch of the Russian Academy of Science, Ekaterinburg, Russia
[6] Ural State University of Railway Transport, Yekaterinburg, Russia
e-mail: rusfive@mail.ru

Received May 30, 2021
Revised September 21, 2021
Accepted September 22, 2021

In present work amorphous alloys $Co_{48}Fe_{25}Si_4B_{19}Nb_4-R$ (R = Nd, Sm, Tb, Yb) were obtained by planar flow casting in the form of ribbons with 3−5 mm wide and 35−45μm thickness. It was found that crystallization process goes into two stages and depends on the used rare-earth addition and its content in the alloy by differential thermal analysis method. Glass-forming ability criteria were calculated. It is shown that paramagnetic Curie temperature of alloys in liquid state can be used as their a-priori criterion of glass-forming ability.

Keywords: amorphous alloys, crystallization, glass-forming ability, differential thermal analysis, x-ray diffraction, rare-earth metals.

DOI: 10.21883/TP.2022.01.52530.165-21

Introduction

Bulk metallic glasses are objects with unique mechanical, magnetic, and corrosion properties [1]. These materials have already found industrial application. Specifically, amorphous rods based on cobalt and iron are used as new highly sensitive sensors [2–4]. However, the applicability of Co-based bulk metallic glasses (BMG) is limited by their relatively poor glass-forming ability. Therefore, the issue of enhancement of their glass-forming ability remains topical.

New BMG have recently been produced in the shape of rods 5.5 mm in diameter with the following compositions: $Co_{46}Fe_{20}B_{22-x}Si_{6-x}Nb_6$ ($x = 0-2$) [5] and $(Co_{1-x}Fe_x)_{68}B_{21.9}Si_{5.1}Nb_5$ ($x = 0.1-0.5$) [6]. According to the authors of these studies, these metal glasses have excellent magnetic properties (the saturation magnetization is as high as 0.49−0.91 T at a coercive force of 0.71−1.58 A/m, and the effective permeability is $(2.21-3.25)\cdot 10^4$ at 1 kHz in a field of 1 A/m). In addition, these cobalt-based BMG are characterized by high values of fracture strength (4250−4450 MPa) and plastic strain (0.6−1.3%) [5–7]. Our earlier studies have revealed [8,9] that the glass-forming ability of cobalt-based alloys may be enhanced by introducing minor quantities of addition elements satisfying the conditions formulated by A. Inoue [1]. The use of other addition elements for enhancing the glass-forming ability of Co- and Fe-based alloys has been discussed in [10,11].

In present study, we added 1 and 2 at.% of rare-earth metals (REMs) Nd, Sm, Tb, Yb to the $Co_{48}Fe_{25}Si_4B_{19}Nb_4$ base composition, examined the crystallization of amorphous ribbons by differential thermal analysis (DTA), and calculated the criteria of glass-forming ability of the indicated alloys.

1. Experimental procedure

Alloys of the $Co_{48}Fe_{25}Si_4B_{19}Nb_4$ composition (master alloy, MA) and with small additions of rare-earth metals (Nd, Sm, Tb, Yb) were produced by remelting of initial components in an induction furnace at 1900 K for half an hour in argon atmosphere.

Amorphous ribbons with a width of 3−5 mm and a thickness of 37−40 μm were obtained by planar flow casting method in controlled argon atmosphere after preparatory overheating of alloys to 1700−1723 K in the induction furnace and subsequent injection to a rotating water-cooled copper whell. Samples were prepared in the shape of ribbons to facilitate the measurement of their electrical resistance and DTA.

The structure of samples was analyzed by X-ray diffraction using a Bruker D8 Advance (CuKα radiation) diffractometer. The crystallization kinetic of amorphous alloys was examined by DTA using a PerkinElmer DTA-7 setup at a heating rate of 10 K/min. Aluminum oxide Al_2O_3 was used as a reference sample. The setup was calibrated in advance to the melting points of pure aluminum and gold. The error of temperature determination was $\pm 1\,K$.

2. Results and discussion

The XRD patterns of MA and alloys in the shape of ribbons with added rare-earth metals are presented in Fig. 1.

It can be seen that all the obtained samples are X-ray amorphous. It was found that the XRD patterns for the samples with neodymium and ytterbium (1 at.%) lack a prepeak located to the left of the primary peak. The same is true for amorphous alloys containing 2 at.% of terbium and ytterbium. The magnitude of the prepeak is the greatest in the alloy with terbium. Alloys with samarium do not have such features. The presence of a prepeak may be indicative both of medium-range ordering in alloys and of the occurrence of microregions enriched in one of the components (i.e., of the microheterogeneity of alloys).

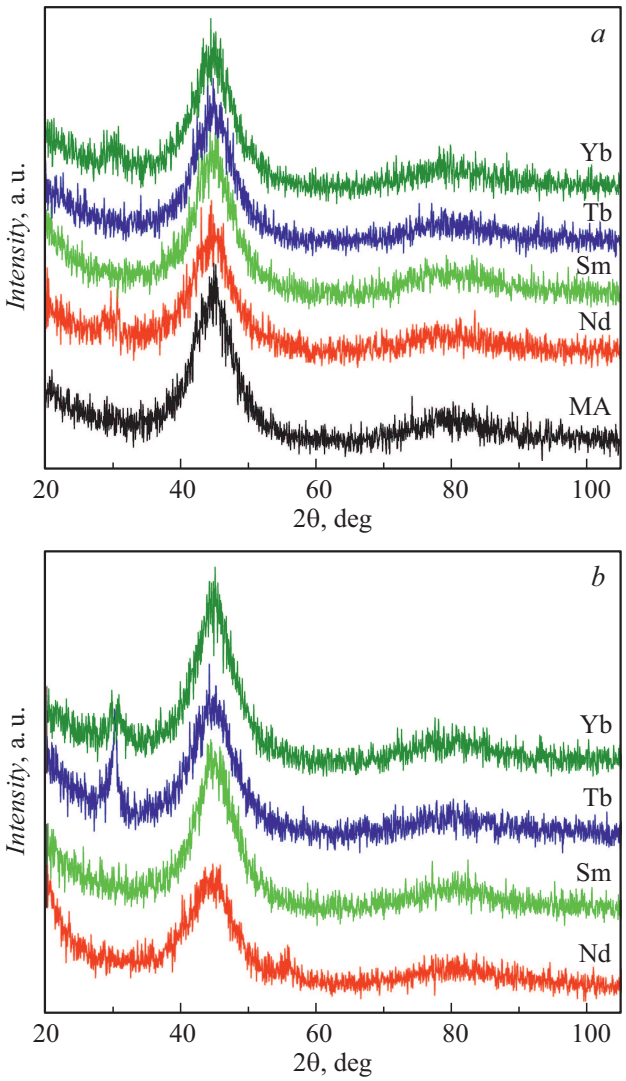

Figure 1. Diffraction patterns of amorphous $Co_{48}Fe_{25}Si_4B_{19}Nb_4$–REM ribbons (REM = Nd, Sm, Tb, Yb). *a* are base composition (MA) and alloys containing 1 at.% REM; *b* are alloys containing 2 at.% REM. The curves are shifted along the vertical axis for clarity.

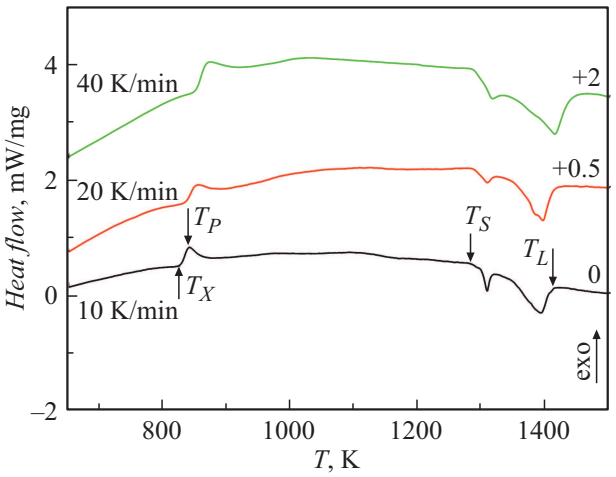

Figure 2. DTA curves of the $Co_{48}Fe_{25}Si_4B_{19}Nb_4$ amorphous alloy measured at different heating rates. Characteristic temperatures T_X (temperature of the onset of crystallization), T_P (peak temperature), T_S (solidus), and T_L (liquidus) are indicated with arrows. Numbers correspond to the magnitude of vertical shift of curves.

Table 1. Characteristic temperatures of the CoFeSiBNb–REM alloys

Alloy	T_{X1}, K	T_{X2}, K	T_S, K	T_L, K
$Co_{48}Fe_{25}Si_4B_{19}Nb_4$–MA	825 ± 1	–	1280 ± 1	1414 ± 1
MA + 1 at.% Nd	841 ± 1	1025 ± 1	1301 ± 1	1398 ± 1
MA + 2 at.% Nd	858 ± 1	994 ± 1	1316 ± 1	1410 ± 1
MA + 1 at.% Sm	833 ± 1	–	1299 ± 1	1394 ± 1
MA + 2 at.% Sm	839 ± 1	–	1298 ± 1	1394 ± 1
MA + 1 at.% Tb	830 ± 1	–	1298 ± 1	1390 ± 1
MA + 2 at.% Tb	846 ± 1	1038 ± 1	1301 ± 1	1393 ± 1
MA + 1 at.% Yb	831 ± 1	1047 ± 1	1296 ± 1	1402 ± 1
MA + 2 at.% Yb	837 ± 1	1042 ± 1	1294 ± 1	1391 ± 1

The crystallization kinetic of amorphous samples was examined by DTA. The curves for the master alloy measured at different heating rates are shown in Fig. 2.

It was found that the base composition features one exothermic reaction in transition from amorphous state to the crystalline one. The process of melting of the base composition occupies a wide temperature interval and involves two endothermic reactions.

The DTA curves for alloys with REM additions are presented in Fig. 3.

It was found that DTA patterns feature one or two exothermic peaks (depending on the REM used). The studied compositions did not reveal glass-transition temperatures (T_g). At the same time, REM additions narrow down the temperature interval of melting $T_L - T_S$ in the studied alloys (this interval for the base composition is 134 K). The characteristic temperatures for the studied alloys are presented in Table 1.

The phase composition of fully crystallized samples was as follows (for the base composition): FCC cobalt

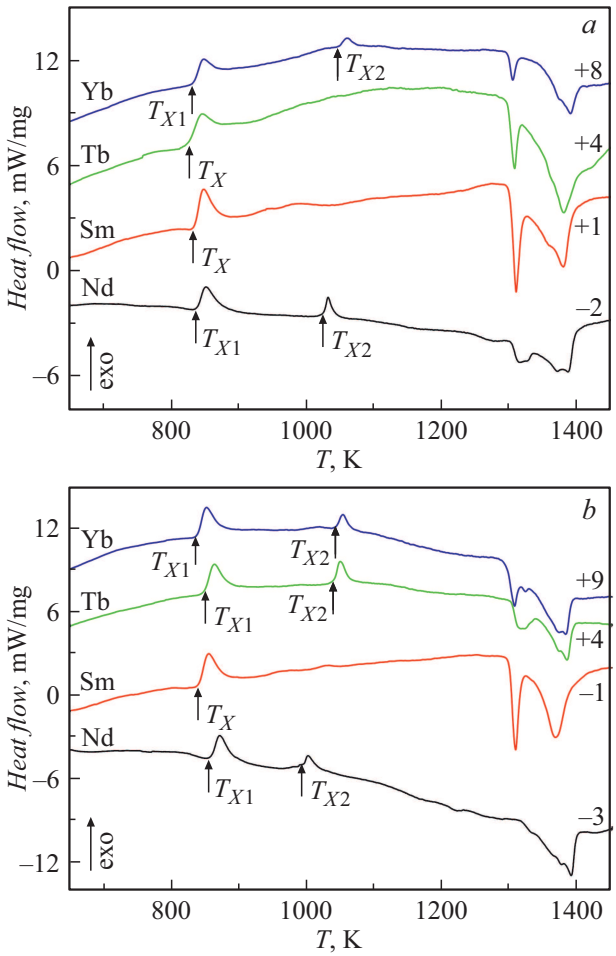

Figure 3. DTA curves of the $Co_{48}Fe_{25}Si_4B_{19}Nb_4$−REM alloys obtained at a heating rate of 10 K/min. *a* are alloys containing 1 at.% REM; *b* are alloys containing 2 at.% REM. Numbers correspond to the magnitude of vertical shift of curves.

and BCC Co−Fe solution (microregions with different concentration) — 52%; oxides (primarily $Fe_{2.2}Co_{0.8}O_4$ and CoO) — 13%; complex ($Fe_3Co_3B_2$, $Fe_3Si_{0.4}B_{0.6}$) and simple (Co_2B, Fe_2B) borides — 29%; metastable phase 23 : 6 (primarily $Co_{11.2}Fe_{9.8}Nb_2B_6$) — 6%.

When rare-earth metals are added, the content percentage of the Co−Fe phase increases significantly (up to 65%), while the content percentage of oxides and borides decreases considerably (4 and 20%, respectively). In addition, REM borides were found in alloys with neodymium and ytterbium and in the alloy with 2% of terbium. Apparently, these borides are produced at temperatures of the second peak in the DTA patterns.

The characteristic temperatures determined experimentally provide an opportunity to calculate certain criteria of glass-forming ability of the studied alloys. A large number of such criteria are known. Since glass-transition temperature T_g was not established in our experiments, we have chosen those criteria that do not include it: $\Delta T_L = T_L - T_X$ [12], $\alpha = T_X/T_L$ [13,14], and $\omega_J = \big(T_L(T_L + T_X)\big)/\big(T_X(T_L - T_X)\big)$ [15]. The results of calculation of the indicated criteria of glass-forming ability are presented in Table 2.

Table 2. Criteria of glass-forming ability of the $Co_{48}Fe_{25}Si_4B_{19}Nb_4$−REM alloys

Alloy	ΔT_L, K [12]	α [13,14]	ω_J [15]	θ, K [16]
$Co_{48}Fe_{25}Si_4B_{19}Nb_4$−MA	589	0.58	6.52	740
MA + 1 at.% Nd	557	0.60	6.68	780
MA + 2 at.% Nd	551	0.61	6.76	800
MA + 1 at.% Sm	561	0.60	6.64	800
MA + 2 at.% Sm	556	0.60	6.68	840
MA + 1 at.% Tb	560	0.60	6.64	760
MA + 2 at.% Tb	547	0.61	6.74	770
MA + 1 at.% Yb	571	0.59	6.60	760
MA + 2 at.% Yb	555	0.60	6.68	780

It should be noted that the existing criteria do not have a predictive ability. One first needs to produce an alloy in an amorphous state, then determine accurately the characteristic temperatures, and only then it becomes possible to calculate the criteria of glass-forming ability. However, the obtained data allow us to conclude that criterion ΔT_L is the most informative of the three calculated ones (it changes significantly after the introduction of addition elements) and that the addition producing a significant increase in T_X is the most efficient. Criteria α and ω_J do not represent clearly the differences between alloys.

Earlier, we have formulated the hypothesis of a-priori determination of glass-forming ability of alloys prone to amorphization based on the examination of their magnetic properties in liquid state and the calculation of paramagnetic Curie temperature (θ) [8,16]. Temperature θ is essentially an exchange integral (i.e., it characterizes the strength of the interatomic interaction in melts). If an addition element produces an increase in θ, it stabilizes the melt structure and interferes with crystallization (i.e., enhances the glass-forming ability). It was hypothesized in [16] that neodymium and samarium are the best addition elements for enhancing the glass-forming ability of the $Co_{48}Fe_{25}Si_4B_{19}Nb_4$−REM alloys. The results presented above verify this hypothesis: amorphous alloys with neodymium and samarium are characterized by a more uniform distribution of elements over the volume and elevated temperatures of cristallization onset.

Conclusion

DTA studies of the $Co_{48}Fe_{25}Si_4B_{19}Nb_4$−REM amorphous alloys demonstrated that all REMs increase the temperature of the onset of crystallization. The calculated criteria of glass-forming ability and data on the paramagnetic Curie temperature allow us to conclude that the hypothesis of applicability of this temperature as a-priori criterion of glass-forming ability was verified.

Acknowledgments

P. Svec Sr. and D. Janickovic acknowledge support for projects VEGA 2/0144/21 and APVV-19-0369.

Conflict of interest

The authors declare that they have no conflict of interest.

References

[1] C. Suryanarayana, A. Inoue. *Bulk Metallic Glasses* (CRC Press, Boca Raton, 2017), DOI: 10.1201/9781315153483
[2] K. Mohri, K. Kawashima, T. Kozhawa, Y. Yoshida, L.V. Panina. IEEE Trans. Magn., **28**, 3150 (1992). DOI: 10.1109/20.179741
[3] L.V. Panina, K. Mohri, T. Uchiyama, M. Noda, K. Bushida. IEEE Trans. Magn., **31**, 1249 (1995). https://doi.org/10.1109/20.364815
[4] H.Q. Guo, H. Kronmuller, T. Dragon, Z.H. Cheng, B.G. Shen. J. Appl. Phys., **89**, 514 (2001). DOI: 10.1063/1.1331649
[5] Q. Man, H. Sun, Y. Dong, B. Shen, H. Kimura, A. Makino, A. Inoue. Intermetall., **18**, 1876 (2010). DOI: 10.1016/j.intermet.2010.02.047
[6] Y. Dong, A. Wang, Q. Man, B. Shen. Intermetall., **23**, 63 (2012). DOI: 10.1016/j.intermet.2011.12.020
[7] Q. Wang, G. Zhang, J. Zhou, C. Yuan, B. Shen. J. Alloys Compounds, **820**, 153105 (2020). DOI: 10.1016/j.jallcom.2019.153105
[8] V. Sidorov, J. Hosko, V. Mikhailov, I. Rozkov, N. Uporova, P. Svec,, D. Janickovic, I. Matko, P. Svec Sr, L. Malyshev. J. Magn. Magn. Mater., **354**, 358 (2014). DOI: 10.1016/j.jmmm.2013.10.038
[9] J. Hosko, I. Janotova, P. Svec, D. Janickovic, G. Vlasak, E. Illekova, I. Matko, P. Svec. J. Non-Crystall. Solids, **358** (*12–13*), 1545 (2012). DOI: 10.1016/j.jnoncrysol.2012.04.016
[10] Z.X. Dou, Y.L. Li, K. Lv, T. Wang, F.S. Li, X.D. Hui. Mater. Sci. Eng.: B, **264**, 114942 (2021). DOI: 10.1016/j.mseb.2020.114942
[11] M. Aykol, M.V. Akdeniz, A.O. Mekhrabov. Intermetall., **19** (9), 1330 (2011). DOI: 10.1016/j.intermet.2011.05.004
[12] Y. Zhang, D.Q. Zhao, M.X. Pan, W.H. Wang. Mater. Sci. Technol., **19** (7), 973 (2003). DOI: 10.1179/026708303225003045
[13] T. Wakasugi, R. Ota, J. Fukunaga. J. Am. Ceram. Soc., **75** (11), 3129 (1992). DOI: 10.1111/j.1151-2916.1992.tb04398.x
[14] K. Mondal, B.S. Murty. J. Non-Cryst. Solids, **351** (16–17), 1366 (2005). DOI: 10.1016/j.jnoncrysol.2005.03.006
[15] X.L. Ji, Y. Pan. Trans. Nonferrous Met. Soc. China, **19** (5), 1271 (2009). DOI: 10.1016/S1003-6326(08)60438-0
[16] B.A. Rusanov, V.E. Sidorov, V.A. Mikhailov, P. Svec Sr., D. Janickovic, Zh. Tekh. Fiz., **91** (8), 1253 (2021) (in Russian). DOI: 10.21883/JTF.2021.08.51100.28-21